IASTED International Conference on Signal and Image Proceesing (SIP-95)
Las Vegas, Nevada. November 20–23, 1995.

# SHAPE RECOVERY FROM NOISY IMAGES BY CURVE EVOLUTION

**Jayant Shah**
**Mathematics Department, Northeastern University, Boston, Mass. 02115**

**Abstract**[1]: *A new approach is presented for recovering shapes from noisy images. First, an edge-strength function,* v, *at every pixel is determined by implementing a segmentation functional. Then, the zero-crossings of the laplacian of the smoothed image are allowed to evolve under the influence of* v. *Each point on the zero-crossings moves in the direction of the normal with a velocity consisting of two components, a component proportional to the directional derivative of* v *in the direction of the normal and a component proportional to curvature. The former pulls the zero-crossings towards the true object boundaries while the latter smooths them, eliminating at the same time extraneous edges. The final result is a representation of the shape outline in the form of a collection of closed curves.*

***KEY WORDS:*** *Shape Recovery, Geodesics, Curve evolution, Segmentation*

## 1. INTRODUCTION

A new approach is developed as a way to exploit the advantages of segmentation methods based on minimizing energy functionals while avoiding at the same time the usual difficulties encountered in their implementation. The main idea is to determine an edge-strength function, $v$, by means of a segmentation functional and then determine the actual boundaries in the form of geodesics defined in a metric determined by $v$. Geodesics are found by choosing an initial curve and letting it evolve to a geodesic. The edge-strength function is reviewed in §2. The equations for curve evolution are derived in §3. In §4, a strategy for choosing the initial curve is discussed while the details of the numerical implementation are given in §5. An illustrative example is described in §6.

## 2. The Edge-Strength Function

Recall the segmentation functional introduced in [2]:

$$E_{MS}(u,B) = \int\int_{R\setminus B} \|\nabla u\|^2 dxdy + \frac{1}{\sigma^2}\int\int_R (u-g)^2 dxdy + \nu|B| \tag{1}$$

where

$R \subset \mathbf{R}^2$ is a connected, bounded, open subset, the "image" domain,
$g$ is the feature intensity, $g : R \to \mathbf{R}$,
$B \subset R$ is a curve segmenting $R$; it is the union of "object" boundaries,
$u$ is the smoothed image which need not be continuous across $B$,
$|B|$ is the length of $B$ and
$\sigma, \nu$ are the weights. ($\sigma$ may be thought of as the smoothing radius.)

Since it is difficult to apply gradient descent with respect to $B$, we follow Ambrosio and Tortorelli [3] and replace $B$ by a new variable $v$ which is defined *continuously* over the image domain $R$ as follows. In the energy functional (1),

$$\text{replace } |B| \text{ by } \frac{1}{2}\int\int_R \left\{\rho\|\nabla v\|^2 + \frac{v^2}{\rho}\right\} dxdy \tag{2}$$

The values of $v$ range between 0 and 1 and thus may be interpreted as the probability for the presence of a discontinuity in the image or the strength of an edge at a given point. An isolated edge may now be represented by $v$ which equals one at the edge and decays exponentially to zero away from the edge. Thus, we may also think of $v$ as a blurred version of $B$ with the blurring radius equal to $\rho$. Since $B$ is now spread out over all of $R$, it is necessary to modify also the smoothing constraint in the energy functional since we no longer have the set $B$. Since smoothing is prevented in the original formulation (1) wherever $B$ is present, a simple choice is:

$$\text{replace } \int\int_{R\setminus B} \|\nabla u\|^2 dxdy \text{ by } \int\int_R (1-v)^2\|\nabla u\|^2 dxdy \tag{3}$$

The corresponding gradient descent equations are:

$$\begin{aligned} \frac{\partial u}{\partial t} &= \nabla\cdot(1-v)^2\nabla u - \frac{1}{\sigma^2}(u-g);\ \frac{\partial u}{\partial n}|_{\partial R} = 0 \\ \frac{\partial v}{\partial t} &= \nabla^2 v - \frac{v}{\rho^2} + \frac{2}{\nu\rho}(1-v)\|\nabla u\|^2;\ \frac{\partial v}{\partial n}|_{\partial R} = 0 \end{aligned} \tag{4}$$

where $\partial R$ denotes the boundary of $R$ and $n$ denotes the direction normal to $\partial R$.

[1] This research was partially supported under NIH Grant No. I-R01–NS34189–01. A more detailed report on the subject of this paper is given in [1].

## 3. CURVE EVOLUTION

Let $\Gamma$ be a simple closed curve in $R$. In order to move $\Gamma$ to where the image intensity gradient and hence $v$ are high, we look for the stationary points of the functional

$$L = \int_{\Gamma} (1-v)^{\alpha} d\gamma \tag{5}$$

where $\gamma$ denotes the arc-length along $\Gamma$. To derive the evolution equation for $\Gamma$, we apply gradient descent to $L$. Let $C(p,t) : I \times [0,\infty) \rightarrow R$ be the evolving family of curves where $I$ is the unit interval and $t$ denotes time. With $x, y$ as the coordinates in the plane, $C(p,t)$ is the vector $\{x(p,t), y(p,t)\}$. We require that $C(0,t) = C(1,t)$ for all values of $t$ and the image of $C(p,0)$ in $R$ coincides with $\Gamma$. The infinitesimal arc length $d\gamma = \lambda dp$ where $\lambda^2 = (\partial x/\partial p)^2 + (\partial y/\partial p)^2$. The velocity of the evolving curve is $\partial C/\partial t = (\partial x/\partial t, \partial y/\partial t)$ which must equal some specified velocity $\beta(p,t)$ along the normal. Therefore, the evolution equation takes the form

$$\frac{\partial C}{\partial t} = \beta(p,t) N \tag{6}$$

where $N$ is the outward normal. Noting that $\frac{\partial v}{\partial t} = \frac{\partial v}{\partial x}\frac{\partial x}{\partial t} + \frac{\partial v}{\partial y}\frac{\partial y}{\partial t} = \nabla v \cdot N\beta$ and $\partial\lambda/\partial t = \beta\kappa\lambda$ where $\kappa$ is the curvature which is defined such that it is positive when $\Gamma$ is a circle,

$$\frac{\partial L}{\partial t} = \int \left[-\alpha(1-v)^{\alpha-1}\nabla v \cdot N + (1-v)^{\alpha}\kappa\right]\beta\lambda dp \tag{7}$$

In order to decrease $L$, we choose

$$\beta = \alpha\nabla v \cdot N - (1-v)\kappa \tag{8}$$

so that the evolution of $\Gamma$ is governed by the equation

$$\frac{\partial C}{\partial t} = [\alpha\nabla v \cdot N - (1-v)\kappa]N \tag{9}$$

The velocity $\beta$ has two terms: the smoothness term represented by the component depending on curvature and advection induced by $v$. The curve is pulled towards the object boundary by the force field $\nabla v$ induced by $v$. The exponent $\alpha$ in the expression for $L$ serves as a weighting factor. The higher the value of $\alpha$, the weaker the smoothing constraint.

In order to implement the evolution of $\Gamma$, assume that $\Gamma$ is embedded in a surface $f_0 : R \rightarrow \mathbf{R}$ as a level curve. Let $f(t,x,y)$ denote the evolving surface such that $f(0,x,y) = f_0(x,y)$. Then, in order to let all the level curves of $f_0$ evolve simultaneously, we consider the functional

$$E = \int_{-\infty}^{\infty} \int_{\Gamma_c} (1-v)^{\alpha} d\gamma_c dc \tag{10}$$

where $\Gamma_c = \{(x,y) | f(t,x,y) = c\}$. But by the coarea formula,

$$E = \int\int_{R} (1-v)^{\alpha} \|\nabla f\| dxdy \tag{11}$$

By calculating the first variation of the last functional, we get the gradient descent equation as

$$\begin{aligned}\frac{\partial f}{\partial t} &= -\alpha\nabla v \cdot \nabla f + (1-v)\|\nabla f\|\nabla \cdot \left(\frac{\nabla f}{\|\nabla f\|}\right) \\ &= -\alpha\nabla v \cdot \nabla f + (1-v)\frac{f_y^2 f_{xx} - 2f_x f_y f_{xy} + f_x^2 f_{yy}}{f_x^2 + f_y^2}\end{aligned} \tag{12}$$

The boundary conditions are:

$$\begin{aligned}\frac{\partial f}{\partial n} &= 0 \text{ along the boundary of } R \\ f &= f_0 \text{ at } t = 0\end{aligned} \tag{13}$$

## 4. ZERO-CROSSINGS AS INITIAL CURVE $\Gamma$

In order for the approach presented here to work, the initial curve should be sufficiently close to the correct boundaries, otherwise, it might converge to a wrong, perhaps spurious geodesic. The strategy is to use zero-crossings of the laplacian as the intial approximation $\Gamma$ for the object boundaries and choose $f_0$ equal to the laplacian of a smoothed version of the image. Now, if the raw image $g$ is very noisy, the laplacian of the smoothed image $u$ obtained from Ambrosio-Tortorelli diffusion will also be very noisy. To see this, consider the behavior of $u$ in the limit as $\rho \rightarrow 0$. In the limit, $u$ is a stationary solution of the original problem (1) and satisfies the differential equation $\nabla^2 u = (u-g)/\sigma^2$, indicating that the laplacian will be as noisy as the original image. It will have many saddle points, indicated by many self-intersections of its zero-crossings. The theory of curve evolution is based on the assumption that $\Gamma$ is a simple closed curve, an assumption which is violated at the saddle points of $f$. If the laplacian is too noisy, the evolution is dominated by what happens at its saddle points and becomes unpredictable. This is because at a saddle point, the first term on the right hand side of the evolution equation (12) vanishes and both the numerator and the denominator vanish in the second term. Hence, the behaviour of the second term becomes very sensitive to noise near a saddle point. Our solution to this problem is to smooth $u$ further by non-uniform smoothing as described below until the zero-crossings of the laplacian have relatively few self-intesections. Recall that we can implement uniform Gaussian smoothing of $u$ by applying gradient descent to the functional

$$\int\int_{R} \|\nabla w\|^2 dxdy \tag{14}$$

In order to reduce the displacement of the significant boundaries (indicated by high values of $v$) due to smoothing, we replace the above functional by the functional

$$\int\int_{R} (1-v)^{\alpha} \|\nabla w\|^2 dxdy \tag{15}$$

The corresponding gradient descent equation is

$$\begin{aligned} \frac{\partial w}{\partial t} &= -\alpha \nabla v \cdot \nabla w + (1-v)\nabla^2 w \\ \frac{\partial w}{\partial n} &= 0 \text{ along the boundary of } R \\ w &= u \text{ at } t = 0 \end{aligned} \tag{16}$$

The diffusion by equation (16) is stopped by the user when the level curves of $\nabla^2 w$ have relatively few self-intesections. Then set $f_0 = \nabla^2 w$ and let it evolve according to equation (12). The zero-crossings of the evolving $f$ are taken as the successive refinements of the object boundaries.

## 5. NUMERICAL IMPLEMENTATION

Implementing the diffusion equations (4) and (16) presents no difficulties since the highest order operator is the laplacian which is very well behaved. Numerical implementation using central differences works quite well. What does require special care is the implementation of the evolution equation (12). The difficulty is that since diffusion is permitted to occur only in the direction of the level curves, the evolution in the direction of $\nabla f$ is governed by the term $\nabla v \cdot \nabla f$. Thus the equation is parabolic in the direction of the level curves and hyperbolic in the direction of $\nabla f$. It is the hyperbolicity which permits the development of shocks, that is, discontinuities which indicate the presence of object boundaries. In the presence of shocks, central finite differences must never be used. One must use forward or backward finite differences adaptively so that their direction is always away from the shock. This principle is expressed by means of the following formuae for calculating $\nabla v \cdot \nabla f$ numerically [4]. For a function $\phi$, let $\phi^n_{i,j}$ denote the value of $\phi$ at the grid point $(i,j)$ at time $n\Delta t$. Let

$$\begin{aligned} D_1^+ \phi^n_{i,j} &= \phi^n_{i+1,j} - \phi^n_{i,j} \\ D_1^- \phi^n_{i,j} &= \phi^n_{i,j} - \phi^n_{i-1,j} \\ D_2^+ \phi^n_{i,j} &= \phi^n_{i,j+1} - \phi^n_{i,j} \\ D_2^- \phi^n_{i,j} &= \phi^n_{i,j} - \phi^n_{i,j-1} \\ D_1 \phi^n_{i,j} &= \left(\phi^n_{i+1,j} - \phi^n_{i-1,j}\right)/2 \\ D_2 \phi^n_{i,j} &= \left(\phi^n_{i,j+1} - \phi^n_{i,j-1}\right)/2 \end{aligned} \tag{17}$$

Then,

$$\begin{aligned} &(\nabla v \cdot \nabla f)_{i,j} \\ &= \max\left(D_1 v^n_{i,j}, 0\right) D_1^- f^n_{i,j} + \min\left(D_1 v^n_{i,j}, 0\right) D_1^+ f^n_{i,j} \\ &+ \max\left(D_2 v^n_{i,j}, 0\right) D_2^- f^n_{i,j} + \min\left(D_2 v^n_{i,j}, 0\right) D_2^+ f^n_{i,j} \end{aligned} \tag{18}$$

The last term in the evolution equation (12) is approximated by central differences while the term $\partial f / \partial t$ is approximated by forward differences.

## 6. ILLUSTRATIVE EXAMPLE

The approach described above is tested on a noisy version of the noiseless image shown in Figure 1a. It consists of 4 squares in the four corners of $R$, a large ellipse in the middle and a long, thin ellipse nearby. The image is represented on a 256×256 square lattice. The thin ellipse has the maximum width of 9 pixels and the distance between the two ellipses is 18 pixels. Figure 1b is a dithered rendition of the noisy version obtained from the image in Figure 1a by adding Gaussian noise with pixel values ranging from 0 to 255. The signal-to-noise ratio (i.e. the ratio between the standard deviation of image with noise removed and the standard deviation of noise) is 1:4. The reason for choosing such an unrealistically low signal-to-noise ratio is the following. The issue is the effect of noise on the placement of the object boundaries. The higher the level noise, the higher the difficulty in finding accurate boundaries, especially when they are sufficiently close to each other to interact. Therefore, in addition to the high level of noise, the example also includes a thin object.

Figure 2 depicts the result of diffusion by equations (4) with $\sigma = \rho = 8$ pixels. The value of $\nu$ was chosen so that highest value of $v$ was nearly equal to 1. In order to ensure numerical stability of the diffusion equations, the time step $\Delta t$ was chosen as 0.1 as it was during the subsequent diffusion steps described below. Figure 2a shows the smoothed image $u$ and Figure 2b depicts the edge strength $v$. The lighter the area, the higher the value of $v$. It is apparent from the figure that thresholding of $v$ will not produce very satisfactory representation of the boundaries. The laplacian of $u$ was so noisy that *almost all the pixels* were zero-crossings of the laplacian. Hence, $u$ was further smoothed by nonuniform diffusion (16) and then the evolution equation (12) was applied to its laplacian. In both the cases, $\alpha$ was set equal to 1 and $v$ was scaled so that its lowest value was 0 and the highest value was 1. Figure 3 shows the effect of the evolving laplacian on its zero-crossings: Figure 3a shows the initial zero-crossings while Figure 3b shows the final zero-crossings.

Figure 4 shows the superposition of the final zero–crossings on the noisefree image (Figure 4a) as well as on the smoothed image $u$ (Figure 4b). Note the accuracy of placement of the smoothed zero-crossings on the noiseless image, including the thin ellipse. The corners are also fairly well represented. The boundary deviates in places from the boundary in the noiseless image where it follows some accidental feature introduced by the noise. (It is possible to discern these features by close inspection of Figure 2a.) It is interesting that although the four corner squares are identical in the noiseless image, the final boundaries are different in all four cases because the accidental noise features are different. The worst deviation occurs in the case of the lower right corner square. The very thin ends of the thin ellipse are lost because our boundary representation $v$ is too coarse ($\rho = 8$ pixels). Some portions

towards the ends of the thin ellipse are lost because they are obscured by noise as one can see in Figure 2a.

## 7. CONCLUSION

Although the results seem promising, the approach described here is in a sense incomplete. A major drawback is that evolution of a single, simple, closed curve cannot represent features such as T-junctions. Another limitation is that the choice of the initial curve involves user interaction. Finally, the edge-strength function and the curve evolution should fit into a single framework to ensure consistency. A hint is provided by the similarity between the functional (11) and the expression (3) of the Ambrosio-Tortorelli approximation, suggesting the following functional for consideration:

$$E_\rho(u,v) = \int\int_R \{\alpha(1-v)^2\|\nabla u\| + \beta|u-g| + \frac{\rho}{2}\|\nabla v\|^2 + \frac{v^2}{2\rho}\}dxdy \tag{19}$$

togetherwith its limit as $\rho \to 0$:

$$E(u,B) = \int\int_{R\setminus B} \|\nabla u\|dxdy + \frac{\beta}{\alpha}\int\int_R |u-g|dxdy + \int_B \frac{J_u}{1+J_u}ds \tag{20}$$

where $J_u$ is the jump in $u$ across $B$, that is, $J_u = |u^+ - u^-|$ where the superscripts + and – refer to the values on two sides of $B$. These functionals will be discussed in a future paper [5].

## 8. REFERENCES


1. J. Shah: "Uses of Elliptic Approximations in Computer Vision", to appear in *Variational Methods for Discontinuous Structures,* Ed: R. Serapioni and F. Tomarelli, Birkhäuser.
2. D. Mumford and J. Shah: "Boundary Detection by Minimizing Functionals, I". Proc. IEEE CVPR, 1985.
3. L. Ambrosio, and V.M. Tortorelli: "On the Approximation of Functionals Depending on Jumps by Quadratic, Elliptic Functionals". Boll. Un. Mat. Ital. 1992.
4. S. Osher and J. Sethian: "Fronts Propagating with Curvature dependent Speed: Algorithms based on the Hamilton-Jacobi Formulation". J. Comp. Physics, 79, 1988.
5. J. Shah: "A Common Framework for Curve Evolution, Segmentation and Anisotropic Diffusion", forthcoming.


FIGURE 1a

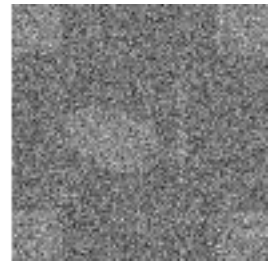

FIGURE 1b

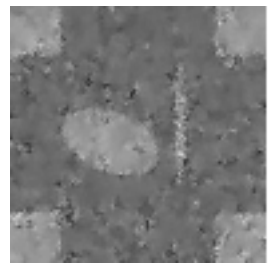

FIGURE 2a

FIGURE 2b

FIGURE 3a

FIGURE 3b

FIGURE 4a

FIGURE 4b